Clim. Past, 10, 1803–1816, 2014
www.clim-past.net/10/1803/2014/
doi:10.5194/cp-10-1803-2014

Climate of the Past
Open Access

Variation in the Asian monsoon intensity and dry–wet conditions since the Little Ice Age in central China revealed by an aragonite stalagmite

J.-J. Yin[1,2,3], D.-X. Yuan[1,2,3], H.-C. Li[1,3,4], H. Cheng[5,6], T.-Y. Li[2], R. L. Edwards[6], Y.-S. Lin[1,3], J.-M. Qin[1,3], W. Tang[3], Z.-Y. Zhao[2,7], and H.-S. Mii[8]

[1]Key Laboratory of Karst Dynamics, MLR and Guangxi, Guilin, Guangxi 541004, China
[2]School of Geographical Sciences, Southwest University, Chongqing 400715, China
[3]Institute of Karst Geology, CAGS, Guilin, Guangxi 541004, China
[4]Department of Geosciences, National Taiwan University, Taipei 10617, Taiwan
[5]Institute of Global Environmental Change, Xi'an Jiaotong University, Xi'an 710049, China
[6]Department of Earth Sciences, University of Minnesota, Minneapolis 55455, USA
[7]Department of Environmental and Resource Sciences, LiuPanShui Normal University, Liupanshui 553004, China
[8]Department of Earth Sciences, National Taiwan Normal University, Taipei 11677, Taiwan

Correspondence to: H.-C. Li (hcli1960@ntu.edu.tw)

Received: 28 February 2014 – Published in Clim. Past Discuss.: 3 April 2014
Revised: 17 August 2014 – Accepted: 24 August 2014 – Published: 1 October 2014

Abstract. This paper focuses on the climate variability in central China since AD 1300, involving:

(1) a well-dated, 1.5-year resolution stalagmite δ^{18}O record from Lianhua Cave, central China

(2) links of the δ^{18}O record with regional dry–wet conditions, monsoon intensity, and temperature over eastern China

(3) correlations among drought events in the Lianhua record, solar irradiation, and ENSO (El Niño–Southern Oscillation) variation.

We present a highly precise, ^{230}Th / U-dated, 1.5-year resolution δ^{18}O record of an aragonite stalagmite (LHD1) collected from Lianhua Cave in the Wuling Mountain area of central China. The comparison of the δ^{18}O record with the local instrumental record and historical documents indicates that (1) the stalagmite δ^{18}O record reveals variations in the summer monsoon intensity and dry–wet conditions in the Wuling Mountain area. (2) A stronger East Asian summer monsoon (EASM) enhances the tropical monsoon trough controlled by ITCZ (Intertropical Convergence Zone), which produces higher spring quarter rainfall and isotopically light monsoonal moisture in the central China. (3) The summer quarter/spring quarter rainfall ratio in central China can be a potential indicator of the EASM strength: a lower ratio corresponds to stronger EASM and higher spring rainfall. The ratio changed from < 1 to > 1 after 1950, reflecting that the summer quarter rainfall of the study area became dominant under stronger influence of the Northwestern Pacific High. Eastern China temperatures varied with the solar activity, showing higher temperatures under stronger solar irradiation, which produced stronger summer monsoons. During Maunder, Dalton and 1900 sunspot minima, more severe drought events occurred, indicating a weakening of the summer monsoon when solar activity decreased on decadal timescales. On an interannual timescale, dry conditions in the study area prevailed under El Niño conditions, which is also supported by the spectrum analysis. Hence, our record illustrates the linkage of Asian summer monsoon precipitation to solar irradiation and ENSO: wetter conditions in the study area under stronger summer monsoon during warm periods, and vice versa. During cold periods, the Walker Circulation will shift toward the central Pacific under El Niño conditions, resulting in a further weakening of Asian summer monsoons.

Published by Copernicus Publications on behalf of the European Geosciences Union.

1 Introduction

The Little Ice Age (LIA; according to Matthes (1939) and Lamb (1977) from ∼ AD 1550 to 1850; hereafter all dates are AD) was the last drift-ice cycle (Bond et al., 2001) characterized by cold conditions (PAGE 2k Consortium, 2013). Due to lower temperatures in the Northern Hemisphere during the LIA, the thermal equator and the rainy belt shifted southward (Broecker and Putnam, 2013), resulting in drier conditions in the Asian monsoon region (Wang et al., 2005; Zhang et al., 2008; Hu et al., 2008; Cui et al., 2012). Conversely, with the current warming, the rainy belt may presumably migrate northward and the monsoonal Asia would in turn become wetter (Broecker and Putnam, 2013). However, several high-resolution and precisely dated speleothem records in the Asian monsoon region (i.e., Zhang et al., 2008; Tan et al., 2009; Burns et al., 2002; Hu et al., 2008; Li et al., 2011; Wan et al., 2011) reveal an excursion of the δ^{18}O toward heavier values over the past several decades that was interpreted as a weak monsoon trend. In fact, the East Asian summer monsoon (EASM) index showed a general decrease trend since 1920 (IPCC, 2007; Wang et al., 2006). If both the cold conditions during the LIA and warm conditions during the Current Warm Period (CWP) resulted in weak EASM on decadal timescales, what are the driving forces for variability of the Asian summer monsoon? Was the summer monsoon precipitation over eastern China lower during the weak EASM periods? Do stalagmite δ^{18}O records in eastern China register "amount effect" of local precipitation? In order to address the above questions, a comparison of high-resolution, well-dated stalagmite δ^{18}O records with instrumental and historic records is required. Few published stalagmite δ^{18}O records were able to compare with instrumental and historic records in eastern China, especially in central China, owing to a lack of precise chronology and interannual resolution. Therefore, the relationships among stalagmite δ^{18}O, Asian monsoon intensity and monsoonal precipitation on annual-to-decadal scales need to be further investigated.

In this study, we establish a new well-dated and high-resolution (∼ 1.5 year) speleothem record from Lianhua Cave, Hunan Province, central China. Based on the record, we probe the relationships among solar irradiation, ENSO, temperature and summer monsoon precipitation and, in turn, the influencing factors for summer monsoon precipitation in central China since 1300.

2 Cave site and local climate conditions

Lianhua Cave (29°09′ N, 109°33′ E; 459 m a.s.l.) is located 36 km south of the Longshan City in the northwestern Hunan Province of central China, and situated in the Wuling Mountain, which is on the south bank of the middle Yangtze River between the Yunnan-Guizhou Plateau and Hunan Basin (Fig. 1). The host rock in the cave site is Upper Ordovician limestone enriched with dolomite. The main cave passage is about 570 m long and connects three main chambers (Fig. 2). The current entrance was found and enlarged during road construction in the late 20th century. In 2011, stalagmite LHD1 was collected in the second chamber, where abundant modern and fossil speleothems existed. The current cave temperature is about 16.3° with relative humidity of > 95 %. Annual mean air temperature and rainfall at Longshan City in the instrumental records are 15.8° and ∼ 1400 mm, respectively.

There are six meteorological stations around Lianhua Cave: Youyang, Sangzhi, Longshan, Laifeng, Enshi and Yichang stations (Fig. 1). In the study area, about 76 % of annual precipitation falls in its rainy season between April and September (calculated from rainfall records of Yichang, Enshi and Youyang between 1951 and 2012) (Fig. 3). After the rainy season, precipitation decreases accordingly in the cave site. The oxygen isotope (δ^{18}O) of precipitation becomes lighter during the rainy season, and reaches the lightest value in July and August (Liu et al., 2010; Cheng et al., 2012; Liu et al., 2014).

Precipitation records from the six stations show essentially consistent variations for the past 60 years (Fig. 4), suggesting that the climate record from Lianhua Cave may reflect wet-dry conditions and regional flooding/drought events of the entire Wuling Mountain area under the influence of the Asian summer monsoon variation. In addition, note that the two precipitation plunges occurred during 1965–1966 and 1982–1983 when a strong El Niño occurred.

3 Sample, methods and results

3.1 Sample description

Stalagmite LHD1 is about 33 cm in height (Fig. 5). We halved the stalagmite along its growth axis. Its mineral composition and possible recrystallization were examined by using X-ray diffraction (XRD) on nine samples throughout the stalagmite at both the University of Science and Technology of China and the University of Minnesota, respectively. The XRD results indicate that the stalagmite is pure aragonite without recrystallization.

3.2 ^{230}Th / U dating and chronology

A total of 25 subsamples 10–100 mg in size for ^{230}Th dating were drilled along the growth axis at different depths, particularly at the top and bottom of each dark layer for potential hiatus. The chemical procedure used to separate uranium and thorium was conducted following Edwards et al. (1987). U and Th measurements were made on a ThermoFinnigan Neptune high-precision multi-collector inductively coupled plasma mass spectrometer (MC-ICP-MS) in the Department of Earth Sciences, University of Minnesota (Cheng et al., 2013). Due to high U (1–6 ppm) and low ^{232}Th contents, the

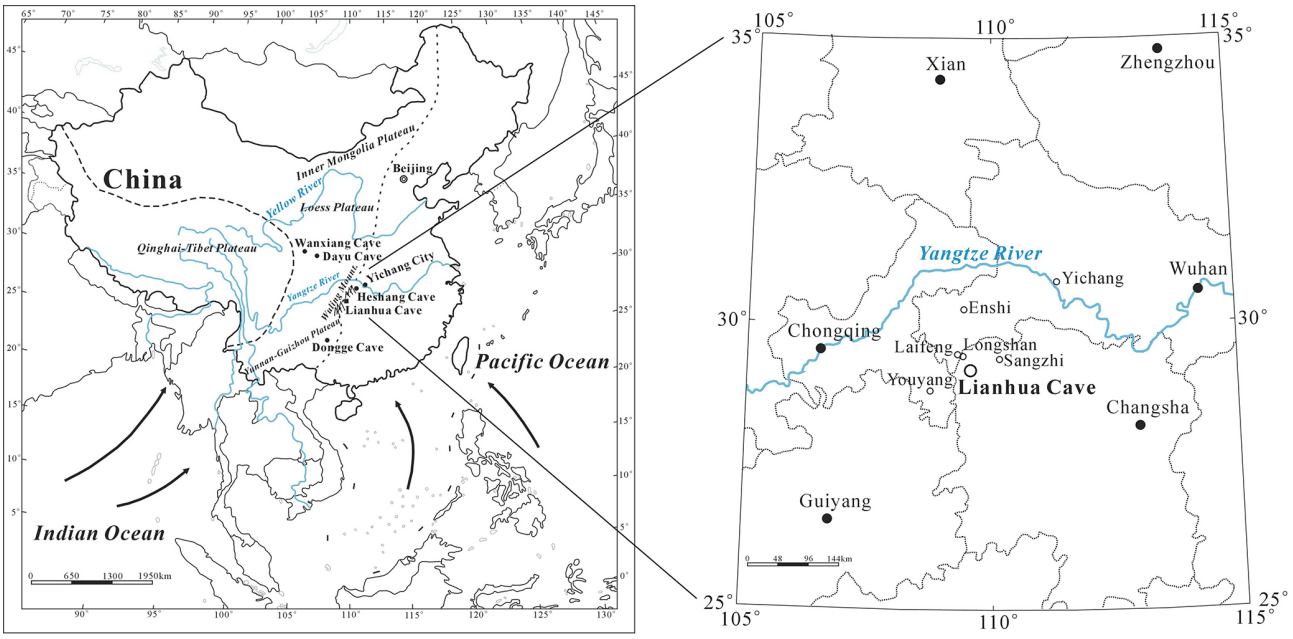

Figure 1. Left: the location of Lianhua Cave. The long-dashed line stands for the boundary of the Qinghai-Tibet plateau in China. The short-dashed line stands for the boundary of the lower plateau and plain in eastern China. Wuling Mountain is located at the boundary between the Yunnan-Guizhou plateau and the eastern plain. Lianhua Cave sits in Wuling Mountain. The arrows denote the direction of moisture source vapor flow from oceans during the summer monsoonal season. Right: meteorological Stations in and around Wuling Mountain. The star symbol indicates the location of Lianhua Cave.

corrections of initial ^{230}Th and dating errors are very small (Table 1).

Based on the 25 ^{230}Th / U dates, stalagmite LHD1 grew continuously from 3290 ± 37 years BP to the present, with an average growth rate of about 0.10 mm yr^{-1}. Linear interpolation method is used to construct the age model (Fig. 5). The top 62 mm covers a time period from 1300 to 2011, which includes the LIA and Current Warm Period (CWP). Except for the top 0.5 mm, the stable isotope resolution of the LHD1 record is about 1.5 years.

3.3 δ^{18}O record

A total of 2995 subsamples for stable isotope analyses were drilled by using a computer-aided triaxial sampler with intervals of 0.1 mm after the first sample, which contains the top 0.5 mm. A total of 543 subsamples used in this study were analyzed on a Finnigan MAT-253 mass spectrometer equipped with a Kiel-III Carbonate Device in the Department of Geosciences at National Taiwan University. The δ^{18}O values reported here are relative to the Vienna PeeDee Belemnite standard and the standard deviation of NBS-19 runs ($n = 358$) is better than 0.08 ‰. In order to make the Hendy test (1971), we took seven subsamples on each of the five layers at depths of 17.5, 86.5, 121, 192.5 and 264 mm with a hand drill. The seven sampling points are $\sim$ 10 mm apart starting from the center. The 35 Hendy test samples were measured by a GasBench III-Micromass IsoPrime IRMS in the Department of Earth Sciences at the National Taiwan Normal University.

Oxygen isotopic value of cave deposits can be influenced by many factors such as δ^{18}O of dripping water, cave temperature, ventilation and evaporation inside the cave, recrystallization and aragonite phase transition, etc. (Hendy, 1971). In order to prove a stalagmite δ^{18}O record as a paleoclimate proxy, the isotopic equilibrium condition of the δ^{18}O record often needs to be demonstrated. Normally, the Hendy test (Hendy, 1971) required a stalagmite to meet two criteria: (1) the δ^{18}O values of the subsamples from the same depositional layer should remain constant; and (2) the δ^{18}O and δ^{13}C values from the same depositional layer should have no correlation. However, this classical Hendy test has recently been questioned by many researchers due to the difficulty in obtaining subsamples from a single growth layer (e.g., Fairchild et al., 2006; Dorale and Liu, 2009; Zhang et al., 2013). Dorale and Liu (2009) pointed out that if the first criterion of the Hendy test is met, there is no need for the second criterion since the δ^{18}O is unchanged, so that no δ^{18}O and δ^{13}C correlation can result. They also clarified that a time-series positive correlation between δ^{18}O and δ^{13}C records of a stalagmite could be normal because climatic conditions may force δ^{18}O and δ^{13}C variations in the same direction (Dorale and Liu, 2009). Therefore, good or bad correlation of a plot of δ^{18}O–δ^{13}C along different depths (a time series) of a stalagmite (which is not the second criterion of

Table 1. ^{230}Th dating results of stalagmite LHD1.

Depth (mm)	^{238}U (ppb)	^{232}Th (ppt)	^{230}Th / ^{232}Th (atomic $\times 10^{-6}$)	δ^{234}U* (measured)	^{230}Th / ^{238}U (activity)	^{230}Th age (yr) (uncorrected)	^{230}Th age (yr) (corrected)	$\delta^{234}U_{Initial}$** (corrected)	^{230}Th age (yr BP) (corrected)
6	3649 ± 8	3471 ± 70	30 ± 1	698 ± 3	0.0017 ± 0.0000	111 ± 1	94 ± 12	698 ± 3	33 ± 12
10	4241 ± 8	9600 ± 193	20 ± 1	692 ± 3	0.0028 ± 0.0001	181 ± 3	142 ± 28	693 ± 3	80 ± 28
16	3242 ± 5	6847 ± 137	41 ± 1	691 ± 3	0.0052 ± 0.0001	338 ± 7	302 ± 27	692 ± 3	240 ± 27
26	5207 ± 6	135 ± 3	4175 ± 100	694 ± 2	0.0066 ± 0.0000	425 ± 3	424 ± 3	695 ± 2	361 ± 3
30	4089 ± 8	1891 ± 38	260 ± 6	692 ± 3	0.0073 ± 0.0001	472 ± 5	464 ± 8	693 ± 3	402 ± 8
40	4573 ± 6	32 ± 2	20272 ± 1057	698 ± 2	0.0087 ± 0.0000	557 ± 3	557 ± 3	699 ± 2	494 ± 3
55	4224 ± 5	107 ± 3	7210 ± 188	690 ± 2	0.0111 ± 0.0000	715 ± 3	715 ± 3	692 ± 2	652 ± 3
70	4532 ± 8	930 ± 19	1030 ± 22	685 ± 3	0.0128 ± 0.0001	832 ± 5	828 ± 5	687 ± 3	766 ± 5
90	5509 ± 7	259 ± 5	5537 ± 117	689 ± 2	0.0158 ± 0.0001	1022 ± 4	1022 ± 4	691 ± 2	959 ± 4
109	2803 ± 3	1404 ± 28	612 ± 12	692 ± 2	0.0186 ± 0.0001	1205 ± 4	1196 ± 7	694 ± 2	1135 ± 7
118.5	5369 ± 7	141 ± 3	12936 ± 284	686 ± 2	0.0206 ± 0.0001	1343 ± 5	1343 ± 5	688 ± 2	1280 ± 5
125	6011 ± 14	2570 ± 52	860 ± 18	685 ± 3	0.0223 ± 0.0001	1452 ± 7	1445 ± 9	687 ± 3	1383 ± 9
140	5430 ± 7	224 ± 5	9899 ± 222	682 ± 2	0.0248 ± 0.0001	1615 ± 6	1615 ± 6	686 ± 2	1552 ± 6
149	4100 ± 11	2442 ± 49	714 ± 14	677 ± 3	0.0258 ± 0.0001	1688 ± 7	1678 ± 10	680 ± 3	1617 ± 10
170	6060 ± 13	2922 ± 59	952 ± 19	678 ± 3	0.0278 ± 0.0001	1822 ± 7	1814 ± 9	682 ± 3	1752 ± 9
175	4190 ± 5	471 ± 10	4097 ± 85	677 ± 2	0.0280 ± 0.0001	1831 ± 7	1829 ± 7	681 ± 2	1766 ± 7
185	3757 ± 5	19 ± 7	95826 ± 38450	675 ± 2	0.0287 ± 0.0001	1882 ± 7	1882 ± 7	679 ± 2	1819 ± 7
195	3047 ± 4	148 ± 3	10099 ± 221	666 ± 2	0.0298 ± 0.0001	1966 ± 8	1965 ± 8	669 ± 2	1902 ± 8
210	4921 ± 11	497 ± 10	5218 ± 108	659 ± 3	0.0319 ± 0.0001	2118 ± 9	2116 ± 9	663 ± 3	2054 ± 9
230	3051 ± 4	19 ± 3	88934 ± 14365	660 ± 2	0.0341 ± 0.0001	2263 ± 8	2263 ± 8	664 ± 2	2200 ± 8
250	4442 ± 7	27 ± 2	98544 ± 6107	652 ± 2	0.0364 ± 0.0001	2428 ± 7	2428 ± 7	657 ± 2	2365 ± 7
260	646 ± 1	535 ± 11	778 ± 17	667 ± 3	0.0391 ± 0.0003	2584 ± 19	2570 ± 22	672 ± 3	2508 ± 22
280	2954 ± 5	73 ± 2	27899 ± 759	674 ± 2	0.0419 ± 0.0001	2762 ± 9	2761 ± 9	679 ± 2	2689 ± 9
302	1185 ± 2	2556 ± 51	346 ± 7	665 ± 2	0.0452 ± 0.0001	2999 ± 10	2961 ± 28	671 ± 3	2900 ± 28
320	3580 ± 6	9379 ± 188	296 ± 6	531 ± 3	0.0471 ± 0.0002	3403 ± 13	3353 ± 37	536 ± 3	3291 ± 37

U decay constants: $\lambda_{238} = 1.55125 \times 10^{-10}$ (Jaffey et al., 1971) and $\lambda_{234} = 2.82206 \times 10^{-6}$ (Cheng et al., 2013). Th decay constant: $\lambda_{230} = 9.1705 \times 10^{-6}$ (Cheng et al., 2013). The error is 2σ error.
* $\delta^{234}U = ([^{234}U / ^{238}U]_{activity} - 1) \times 1000$. ** $\delta^{234}U_{initial}$ was calculated based on ^{230}Th age (T), i.e., $\delta^{234}U_{initial} = \delta^{234}U_{measured} \times e^{\lambda 234 \times T}$. Corrected ^{230}Th ages assume the initial ^{230}Th / ^{232}Th atomic ratio of $4.4 \pm 2.2 \times 10^{-6}$. Those are the values for a material at secular equilibrium, with the bulk earth ^{232}Th / ^{238}U value of 3.8. The errors are arbitrarily assumed to be 50 %. B.P. stands for "Before Present" where the "Present" is defined as the year 1950.

the Hendy test, e.g., Fig. 3 in Cosford et al., 2008) is not related to isotope equilibrium conditions. Thus, although the Hendy test is difficult in practice because of extraction of the same material from a single growth layer, the first criterion of the Hendy test is still valid for checking δ^{18}O variation within a sampling layer. Our Hendy test results indicate that the center part of the stalagmite has relatively constant δ^{18}O values. Within the sampling area (3 mm) for the stable isotope record, the variations of the δ^{18}O are normally less than 0.05 ‰ in the five Hendy test layers (Supplement Fig. S1).

Another way to check whether stalagmite carbonates were formed in isotopic equilibrium with cave drip waters is to use modern cave temperatures, δ^{18}O of drip water, and δ^{18}O of modern carbonate deposit under isotopic equilibrium conditions (McDermott, 2004). Modern carbonate deposits and drip waters were collected during the sampling of stalagmite LHD1. The δ^{18}O value of drip water is -6.19 ‰ (VSMOW), and the δ^{18}O of modern speleothem deposit is -5.17 ‰ (VPDB). Using these values, we calculate depositional temperature under isotopic equilibrium using the following equation: $1000 \ln\alpha = 18.56\ (10^3/T) - 32.54$ (Thorrold et al., 1997). The calculated temperature is 15.7 °C, which is similar to the measured cave temperature of 16.3 °C and the mean annual air temperature at the Longshan station.

Recently, replication test has been considered as a best approach for evaluating isotopic equilibrium conditions of cave carbonate deposition (Dorale and Liu, 2009). The replication test requires similar isotopic profiles from two or more stalagmites in a cave. Theoretically, if the kinetic effect of isotopic fractionation is absent, and vadose-zone processes at different dripping sites are the same, one may find the replicated δ^{18}O records in the cave. However, due to the spatial heterogeneity of cave systems and age-dating uncertainty of stalagmites, replication test is not an easy task. For Lianhua Cave, two aragonite stalagmite δ^{18}O records, A1 (Cosford et al., 2008, 2009) and LH2 (Zhang et al., 2013), had been published before. In the comparison of A1 and LH2 regarding their overlapping growth period from 0.05 to 6.5 ka BP, Zhang et al. (2013) found that it was difficult to access the replication test between stalagmite LH2 and A1, perhaps due to isotopic drifts of the A1 δ^{18}O record caused by the LA–GC–IRMS (laser ablation–gas chromatography–isotope ratio mass spectrometry) measurement. Therefore, Zhang et al. (2013) compared LH2 records with Sanbao Cave δ^{18}O records to demonstrate isotopic equilibrium condition. Our analytical method for stable isotopes is the same as that of Zhang et al. (2013). Hence, we can perform the replication test using LHD1 records (this study) and LH2 records (Zhang et al., 2013). In Fig. 6, the LHD1 and LH2 δ^{18}O records show similar variations between 1540 and 1900. Between 1300 and 1540 , the two records show similar variation patterns, but have a $\sim$ 40-year lag. Our record contains 543δ^{18}O

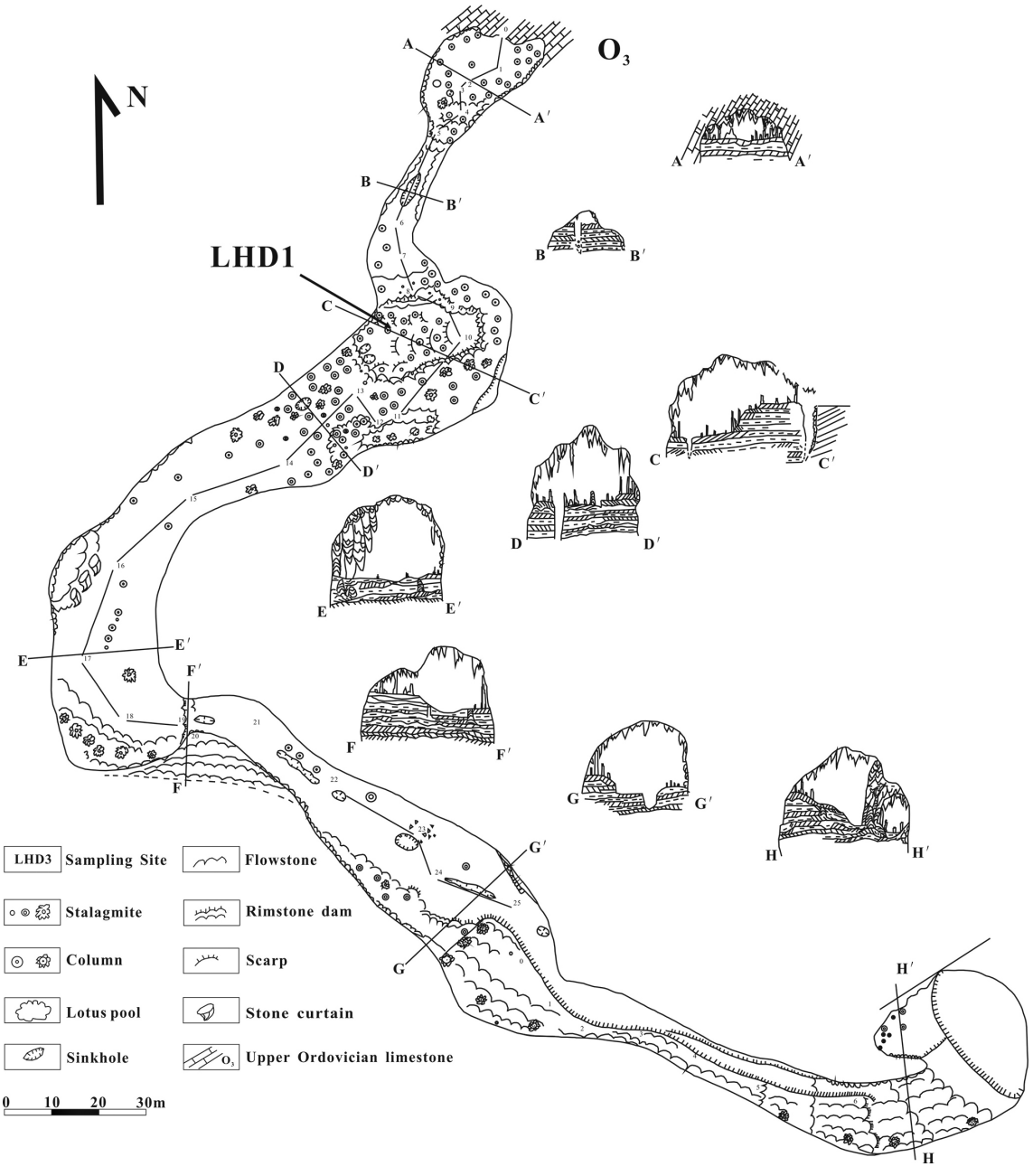

Figure 2. Schematic map of Lianhua Cave. Stalagmite sample LHD1 was collected in the second chamber.

measurements and 7 ^{230}Th / U dates covering the period from 1300 to 2003, whereas the LH2 record has 48 δ^{18}O measurements and 5 ^{230}Th / U dates spanning from 1300 to 1899. Our well-dated and high-resolution record is suitable for comparison with instrumental and historic records.

The δ^{18}O values of the LHD1 record range from −5.04 to −6.75 ‰ (average −5.80 ‰) throughout the past 700 years and are characterized by multi-decadal to centennial oscillations (Fig. 7). The average δ^{18}O value between 1300 and 1850 (in the LIA) is −5.82 ‰, actually undistinguishable from the average value of the whole record. In general, most δ^{18}O values from 1370 to 1580 were lighter than the average value. The δ^{18}O values between 1580 and 1850, which spans the LIA, were heavier than the average value, with the heavy values centered at 1640, 1690 and 1780. The δ^{18}O values between 1850 and 1950 were lighter than the average. Since 1950, the δ^{18}O has shifted toward heavy values, with the heaviest value of −5.04 ‰ in the present (Fig. 7).

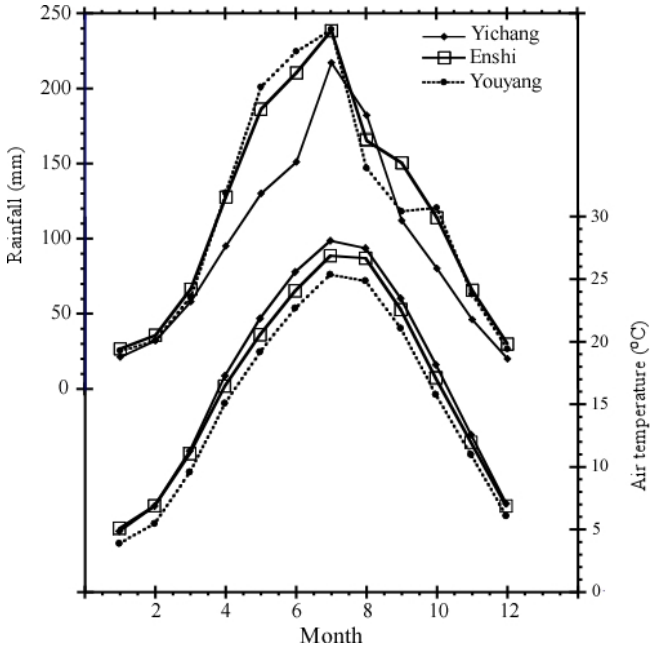

Figure 3. Monthly rainfall and air temperature of the cities around Lianhua Cave. The locations of the cities are shown in Fig. 1 (data from http://cdc.cma.gov.cn).

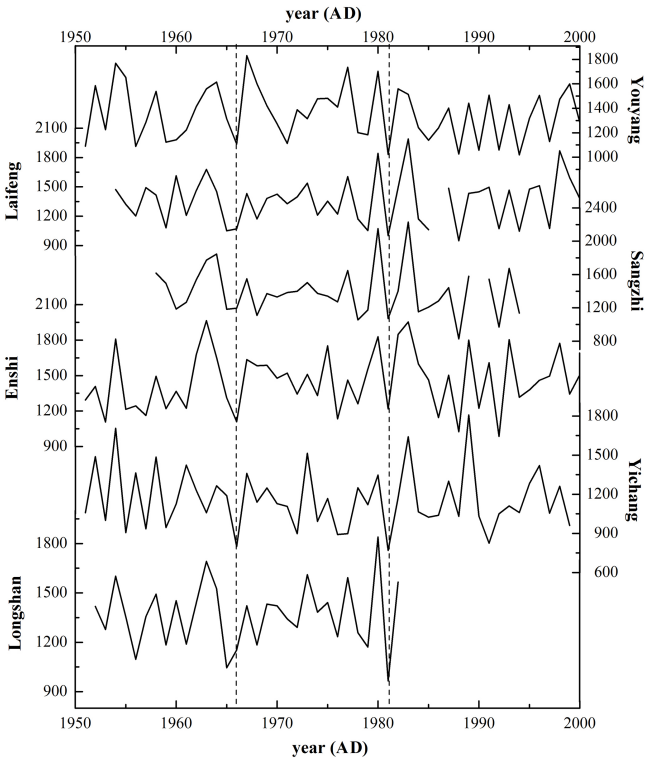

Figure 4. Annual precipitation recorded by meteorological stations around Lianhua Cave (Data from http://cdc.cma.gov.cn). The vertical short-dashed lines showed that two precipitation plunges occurred during 1965–1966 and 1982–1983 when a strong El Niño occurred.

4 Discussion

4.1 Comparison of the δ^{18}O record with weather records

The link between cave δ^{18}O records and climate variation is in general complex, as δ^{18}O of stalagmite is a function of cave temperature and δ^{18}O of dripping water which, in turn, is influenced by rainfall amount, air temperature, moisture source, summer/winter rain ratio, etc. (Wan et al., 2011). Changes in the summer monsoon intensity will affect several factors listed above (Li et al., 1998). In order to understand the effect of climatic factors in terms of rainfall, air temperature and seasonality on stalagmite δ^{18}O change, we compare stalagmite LHD1 δ^{18}O with the local instrumental weather records. In the Wuling Mountain and adjacent areas, precipitation is mostly affected by the Asian summer monsoon, and as aforementioned they show similar regional patterns (Figs. 3 and 4). Because of this reason, we select the Yichang weather record to compare with our Lianhua record, as this record is the longest (from 1882 to 2012 for precipitation and from 1905 to 2012 for temperature) (Fig. 8) (data source: Tao et al., 1997; http://cdc.cma.gov.cn). The data from 1939 to 1946 was missing due to World War II. In order to see major changes of the weather parameters, we use 5-year running average records for all weather records.

Figure 8 shows that the Lianhua δ^{18}O record is generally comparable to the annual rainfall record of Yichang City before 1978, except for the period of 1910∼1930: lighter

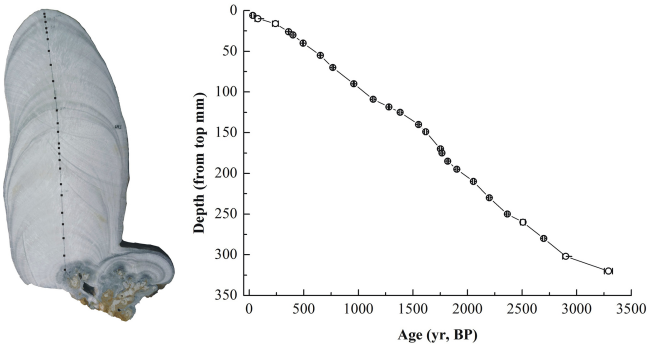

Figure 5. Photo and age model of stalagmite LHD1. Linear interpolations between two adjacent ^{230}Th dates were used.

δ^{18}O value corresponding to higher rainfall and vice versa, which can be explained by the "amount effect". Regardless of the age uncertainty of the δ^{18}O record, we plot correlations between the δ^{18}O and rainfall (P), and between the δ^{18}O and air temperature (T) for the four periods of 1880–1910, 1910–1930, 1930–1978 and 1978–2003. Although the correlations are not strong, the δ^{18}O-P plots have negative slopes during 1880–1910 and 1930–1978, but positive slopes during 1910–1930 and 1978–2003 (Fig. 9). The positive

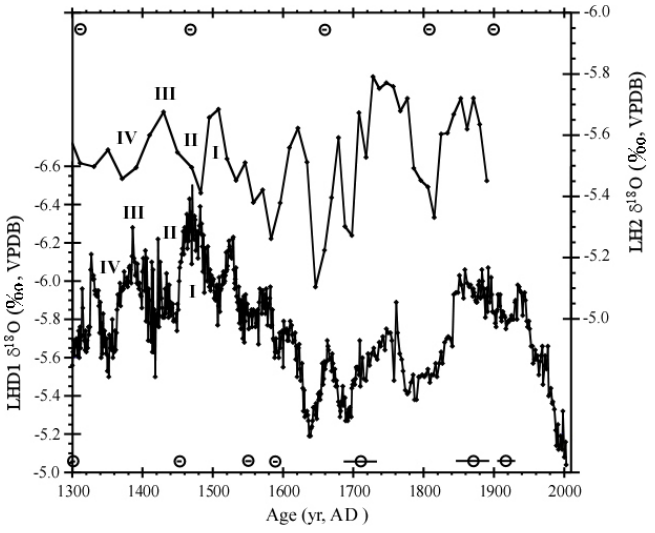

Figure 6. Comparison of the δ^{18}O records between stalagmite LH2 (Zhang et al., 2013) and stalagmite LHD1 (this study). The roman letters denote possible matches with age uncertainty.

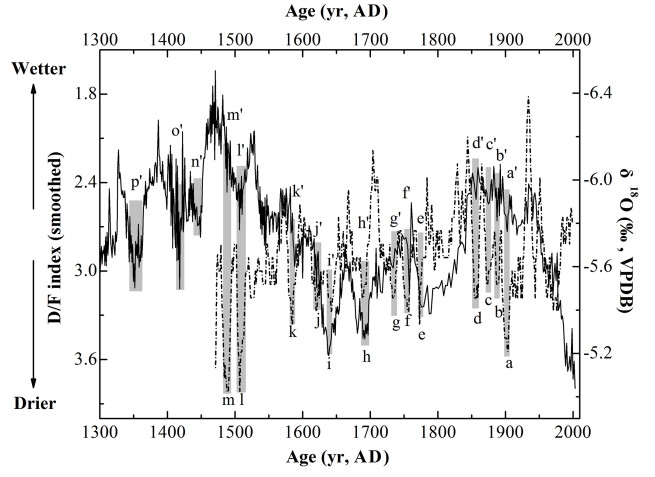

Figure 7. The δ^{18}O record of stalagmite LHD1 (solid line), and its comparison with the drought/flood index of Yichang City (dashed line) (CAM, 1981) (11 years smoothed). Grey bars and the letters were the drought events found in both records.

slopes must be explained by other factors rather than the "amount effect". During the period 1910–1930, the δ^{18}O varied between -5.89 and -5.75 ‰ (VPDB), and rainfall variation had the opposite trend of the temperature change ($P = 18.4 - 0.0122T$, $R^2 = 0.71$). Cave temperature is generally close to the annual mean air temperature above the cave. One degree higher in air temperature (hence higher cave temperature) will cause ~ 0.23 ‰ lighter stalagmite δ^{18}O during carbonate precipitation (Thorrold et al., 1997). In addition, δ^{18}O of rain in typical monsoonal areas of China has a negative correlation with air temperature (Johnson and Ingram, 2004; Li et al., 2007), which means that higher air

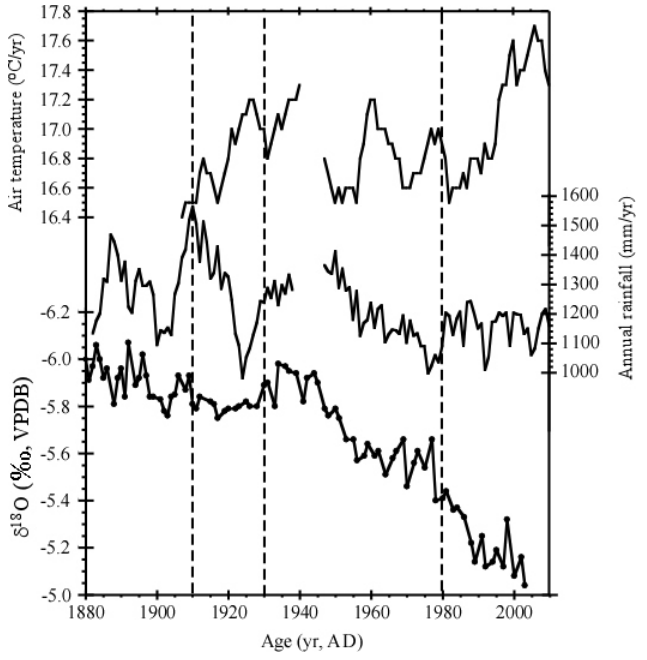

Figure 8. Comparison of stalagmite LHD1 δ^{18}O record with the instrumental weather records of Yichang City. The temperature and rainfall records are 5-year running averages. The dashed lines separate four periods which have different relationships among the stalagmite δ^{18}O, rainfall and air temperature shown in Fig. 9.

temperature corresponds to lighter δ^{18}O in rain. Under such circumstances, a drier climate would result in heavier stalagmite δ^{18}O, but the warmer conditions could tend to cancel out the δ^{18}O shift. Therefore, the opposite effect of rainfall and temperature might obscure the "amount effect" during the 1910–1930 period.

The positive excursion of the δ^{18}O after 1978 is irrelevant with the annual rainfall, but has a positive relationship with annual mean air temperature (Fig. 9). The δ^{18}O values of this period are very heavy. This heavy δ^{18}O trend was not attributed to "amount effect" or temperature effect. The third major effect on speleothem δ^{18}O besides rainfall amount and temperature effect is δ^{18}O of moisture source. In the monsoonal region of eastern China, the δ^{18}O of moisture source during the summer months is lighter than that during the winter season (Li et al., 1998, 2007; Johnson and Ingram, 2004; Liu et al., 2010, 2014). Recently, studies on the monsoonal moisture vapor indicate that the δ^{18}O of moisture source from Indian Ocean may be lighter than that of the moisture source from the Pacific (Pausata et al., 2011; Tan et al., 2007, 2011). Hence, changes in the mixing ratio of winter and summer rainfall and in moisture source domain between the Indian and Pacific oceans will affect stalagmite δ^{18}O. Figure 10 shows the comparison of the stalagmite δ^{18}O with the Yichang rainfall in different seasons. The summer rainfall includes precipitation from May to August, whereas the winter rainfall sums up the precipitation

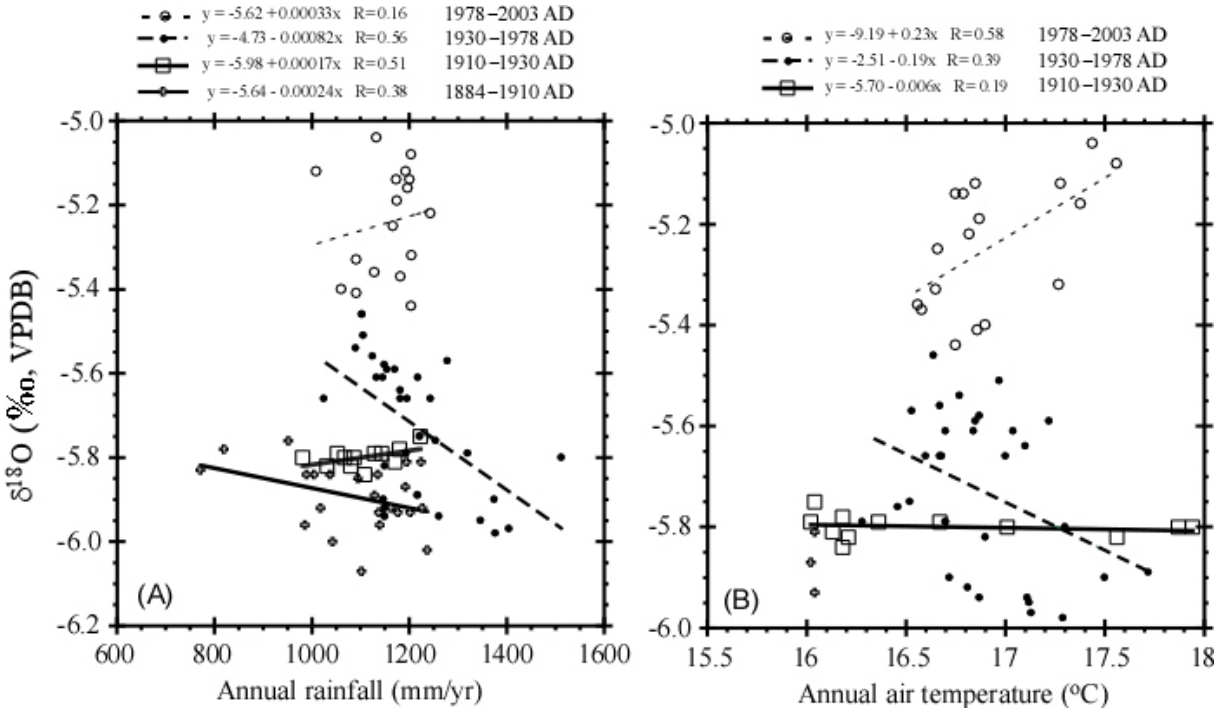

Figure 9. (a) Correlations between δ^{18}O values and Yichang rainfall during the 1884–1910, 1910–1930, 1930–1978 and 1978–2003. **(b)** Correlations between δ^{18}O values and Yichang air temperature during 1910–1930, 1930–1978 and 1978–2003.

in November and December as well as January and February of the next year. The correlation between summer rainfall and winter rainfall is very weak ($R = 0.134$), but both summer and winter rainfalls are positively correlated with the annual rainfall ($R = 0.71$ and $R = 0.61$, respectively). Interestingly, the variation of summer / winter rainfall ratio is dominated by the winter rainfall changes (Fig. 11a). Nevertheless, Figure 10 indicates that the annual summer rainfall after 1978 did not decrease, and the summer / winter rainfall ratio has decreased since 1950, while the δ^{18}O became heavier. Therefore, changes in the mixing ratio of winter and summer rainfall could not explain the positive excursion of the δ^{18}O after 1978.

We further separate the warm season rainfall into the spring quarter (from April to June) and the summer quarter (from July to September), and investigate the moisture source of the rainfall at different quarters. It was known that the period of 1968–1978 had strong EASM, and the period of 1979–1998 had weaker EASM (Qian et al., 2007). During the strong EASM period, the Northwestern Pacific High (NWPH) became weak and shifted northeastward, so that the Intertropical Convergence Zone (ITCZ) was dominant in the monsoonal region of eastern China. The moisture source during the strong EASM period was mainly from the southern Indian Ocean (Zhou and Yu, 2005). Since the moisture source from the Indian Ocean travels a longer distance and experiences more isotopic fractionation, the moisture vapor will have a lighter δ^{18}O value compared with the moisture vapor from the western Pacific (Tan et al., 2011). In Fig. 10, Rainfall in the spring quarter (April–June) during the strong EASM period (1968–1978) was higher than rainfall in the summer quarter (July–September) with low July–September / April–June precipitation ratio. The situation was reversed during the weak EASM period of 1978–1998 (Fig. 10). Indeed, the δ^{18}O became lighter during 1968–1978, and turned to very heavy during 1979–1998. In addition, one can clearly see that the July–September/April–June precipitation ratio was less than 1 before 1950 and became greater than 1 after 1950, which indicates that the subtropical monsoon controlled by the NWPH became more dominant after 1950. The general increasing trend of the July–September / April–June precipitation ratio has been consistent with the weakening of the EASM strength since 1920 (IPCC, 2007). In Fig. 11b, the July–September / April–June precipitation ratio is strongly positively correlated with the summer quarter rainfall, but strongly negatively correlated with the spring quarter rainfall. The annual rainfall has significantly positive correlation with the spring quarter rainfall ($R^2 = 0.5$), but no correlation with the summer quarter rainfall.

In summary, when the spring quarter rainfall of the study area is high, the EASM seems stronger, and the annual rainfall is higher. During the strong EASM, the tropical monsoon trough, controlled by the ITCZ, is dominant in the monsoonal region of eastern China, while the subtropical monsoon is weak, caused by the northeastward retreat of the NWPH. The

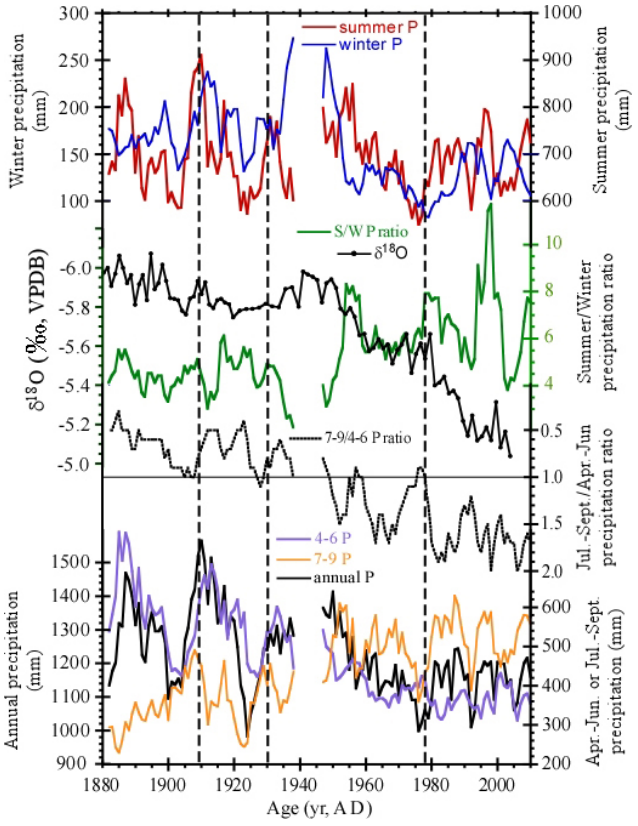

Figure 10. Comparison of the stalagmite LHD1 δ^{18}O record with the seasonal rainfall of Yichang City. Note that the axis of April–June rainfall and July–September rainfall are inversely plotted. Winter precipitation includes rainfall from November to the following February, whereas the summer precipitation sums rainfall from May to August (data source: Tao et al., 1997 and http://cdc.cma.gov.cn).

moisture source to the study area is chiefly from the Indian Ocean, with more depleted δ^{18}O. Thus, both "amount effect" and moisture source effect will result in a lighter stalagmite δ^{18}O shift during the stronger EASM period. One may accept that a heavy δ^{18}O execution in the LHD1 record reflects drier conditions under a weak summer monsoon and higher summer quarter/spring quarter rainfall ratio.

To further understand the Lianhua record beyond the instrumental record, we have compared the δ^{18}O record of LHD1 with a drought/flood index since 1470, reconstructed from historic documents in Yichang area (Fig. 7) (CAM, 1981; Zhang et al., 2003). The historical record reveals 13 drought events, 1491–1493 (m), 1502 (l), 1585–1590 (k), 1616–1618 (j), 1637–1643 (i), 1689–1692 (h), 1729–1737 (g), 1756–1768 (f), 1784–1786 (e), 1856–1858 (d), 1876–1878 (c), 1886–1891 (b), and 1896–1903 (a), which can be seen in the δ^{18}O record of LHD1 (Fig. 7). Among those events, events (a), (b), (c), (d), (g), (h) and (i) affected more than 4 provinces with a duration of 3 years or more (Zhang, 2005); and events (c), (f), and (i) plus an event in 1790–1796 were reported previously as megadrought events in the Asian monsoon region due to Asian summer monsoon failure (Cook et al., 2010). Although the drought event (e) in the Yichang drought/flood index record is significant, it appears neither in the Lianhua record nor in any records in Asian monsoon region to our knowledge. In summary, it seems that the δ^{18}O record of LHD1 can be used as a climatic proxy to indicate major drought events under weak EASM in central China.

4.2 Solar radiation influence and teleconnection to ENSO

It has been well demonstrated that the Asian monsoon changes were dominantly controlled by Northern Hemisphere summer insolation on an orbital timescale and the teleconnection with the North Atlantic climate on a millennial timescale (Wang et al., 2001 and 2008; Cheng et al., 2009, 2012). However, the cause of monsoon changes on annual- to decadal scales and its relation to climatic conditions (e.g., the short-term drought events revealed in our Lianhua record) need to be further explored. Here, we compare the δ^{18}O record of LHD1 with solar irradiation change (Fig. 12). Figure 12 exhibits that negative executions of δ^{18}O generally corresponded to an increase of solar irradiation, and more positive executions of δ^{18}O occurred during solar minima, including Spörer, Maunder, Dalton and 1900 minimum. This is because the temperature change in eastern China was remarkable following the solar irradiation (Fig. 12). It is well known that high continental temperature will enhance land–sea thermal contrast and in turn intensify the summer monsoon (e.g., Kutzbach, 1981). Intensified summer monsoon may be associated with a stronger and larger atmospheric circulation that may transfer more remote moisture from the tropical oceans to the land, resulting in lighter δ^{18}O of rainfall due to fractionation during moisture transportation (Cheng et al., 2012). The correlation between the Lianhua δ^{18}O record and eastern China temperature (Wang et al., 2007; Shi et al., 2012) shows a significantly negative correlation between 1548 and 1937 ($\delta^{18}\mathrm{O} = -6.20 - 1.30 * T$, $r^2 = 0.44$, $n = 253$). When solar irradiation decreased, temperature in eastern China became colder, which in turn led to weaker summer monsoons and resulted in heavier δ^{18}O in the stalagmite. Warmer conditions under increased solar irradiation would enhance the summer monsoon and brought about wetter conditions in the study area.

However, solar irradiation and temperature alone are in sufficient to explain all the drought events in our record. For instance, during the periods of positive shifts (a), (b), (c) and (d) in the δ^{18}O of LHD1 record, solar irradiation and eastern China temperature did not show significant decrease (Fig. 12). Some other mechanisms must be involved. Comparison of our record to the El Niño 3.4 index (Cook et al., 2008) shows that many drought events (positive executions of the δ^{18}O) occurred under the El Niño condition

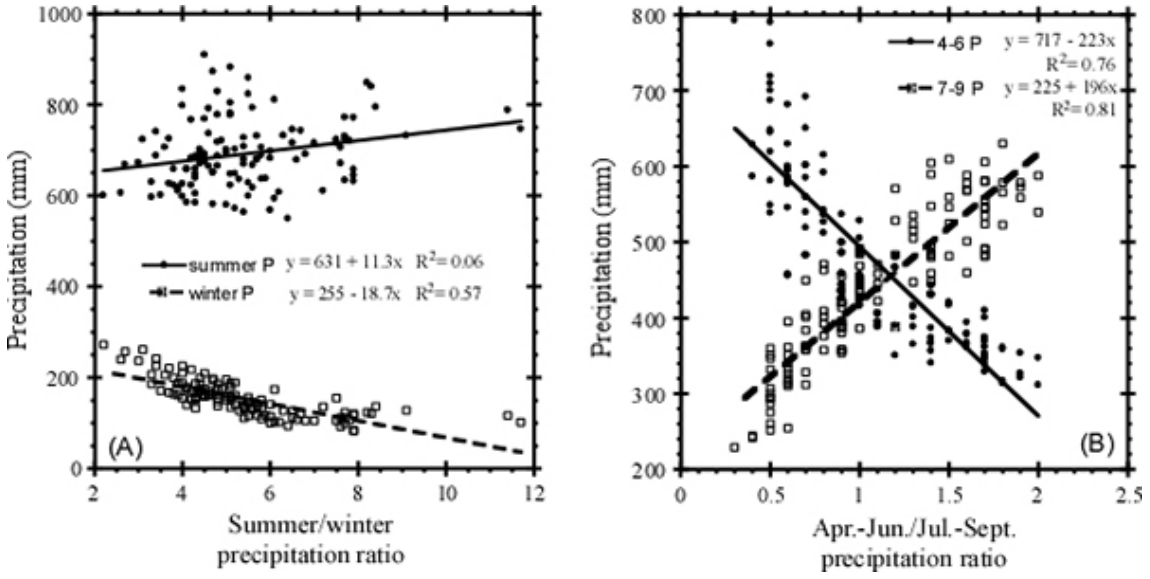

Figure 11. Correlations between seasonal rainfalls and their ratio: **(a)** for winter and summer seasons; and **(b)** for the second (April–June) and third (July–September) quarters.

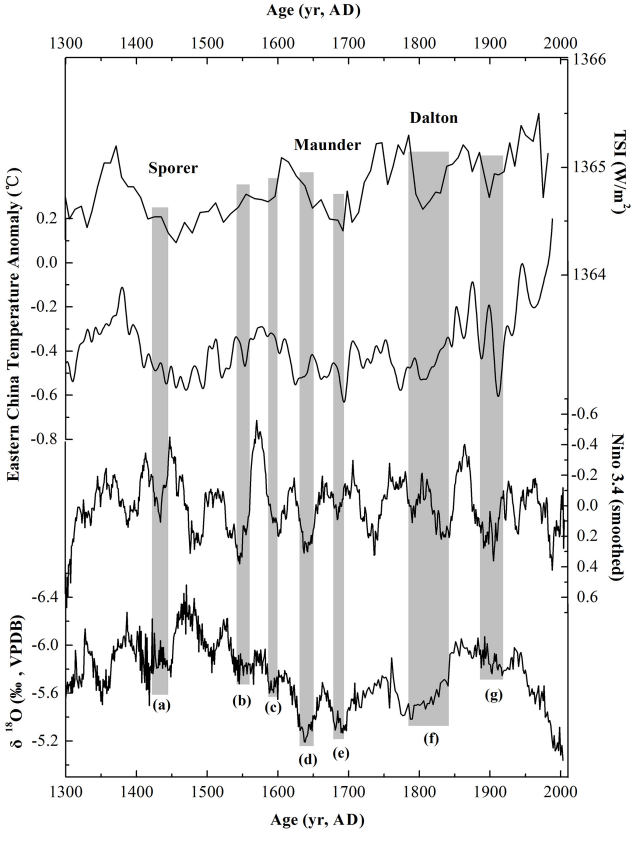

Figure 12. Comparison of δ^{18}O of stalagmite LHD1 with total solar irradiation (Delaygue and Bard, 2011), eastern China temperature (Shi et al., 2012), and Niño 3.4 index (20 years smoothed) (Cook et al., 2008). The grey bars were drought events found in stalagmite LHD1.

(Fig. 12), implying a possible linkage between the drought events and ENSO variations. During El Niño conditions, the Walker Circulation shifted toward the center Pacific, and the sea surface temperature on the tropical western Pacific became cooler. Consequently, the East Asian summer monsoon could be weaker. Note that when solar irradiation was strong, the δ^{18}O became lighter, even during strong El Niño conditions, e.g., during 1340–1400, 1720–1780 and 1920–1950 (Fig. 12). This means that under warm stages when the solar irradiation was strong, the effect of ENSO variation on the East Asian summer monsoon strength was small.

During 1410–1530, eastern China temperature was low, corresponding to the Spörer solar minimum. For this period, the δ^{18}O record was influenced by ENSO conditions, with lighter δ^{18}O corresponding to the La Niña conditions and heavier δ^{18}O corresponding to the El Niño conditions (Fig. 12). It is possible that the strong La Niña conditions led to more moisture source from the Indian Ocean, which had lighter δ^{18}O to reach the study area, instead of heavy rainfall. It seems that during cold stages, the influence of ENSO conditions became dominant.

A power spectrum analysis (Schulz and Mudelsee, 2002) of the Lianhua δ^{18}O time series shows significant periodicities of 2.6–2.7 years (excess 95 % confidence levels), 3.4–4.1 years (excess 80 % confidence level) and 47 years (excess 95 % confidence levels) (Fig. 13). The periodicities of 2.7 and 4.1 years can be seen in the spectrum analysis of Niño 3.4 record (Fig. 13), and is considered as one periodicity of ENSO variability. The 47-year periodicity matches with the 44-year cycle of solar activity, which has also been shown in other cave records in the Asian monsoon region, for example, in Dongge Cave (Dykoshi et al., 2005; Kelly et al., 2006) and

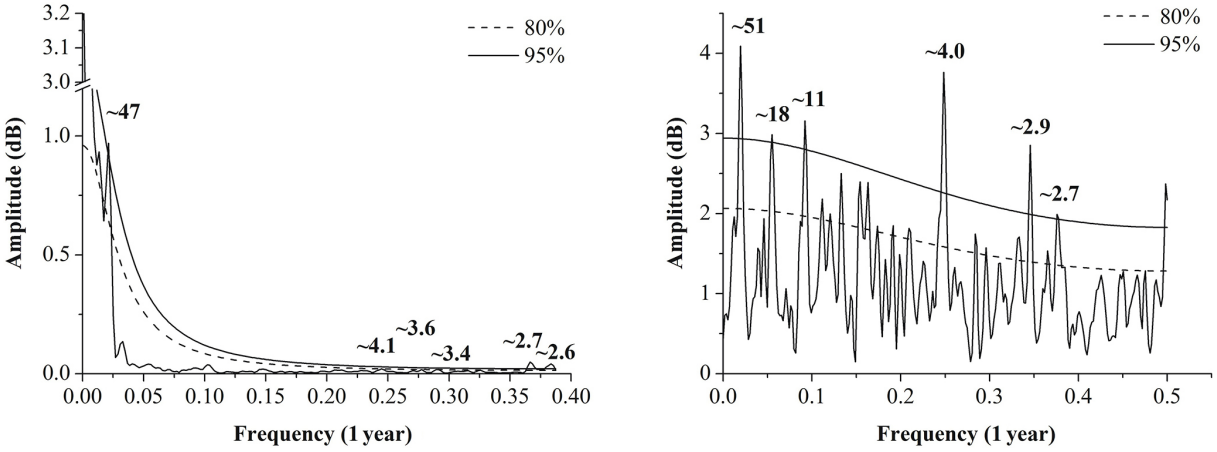

Figure 13. Spectrum analysis of stalagmite LHD1 δ^{18}O record (left) and Niño 3.4 index (right).

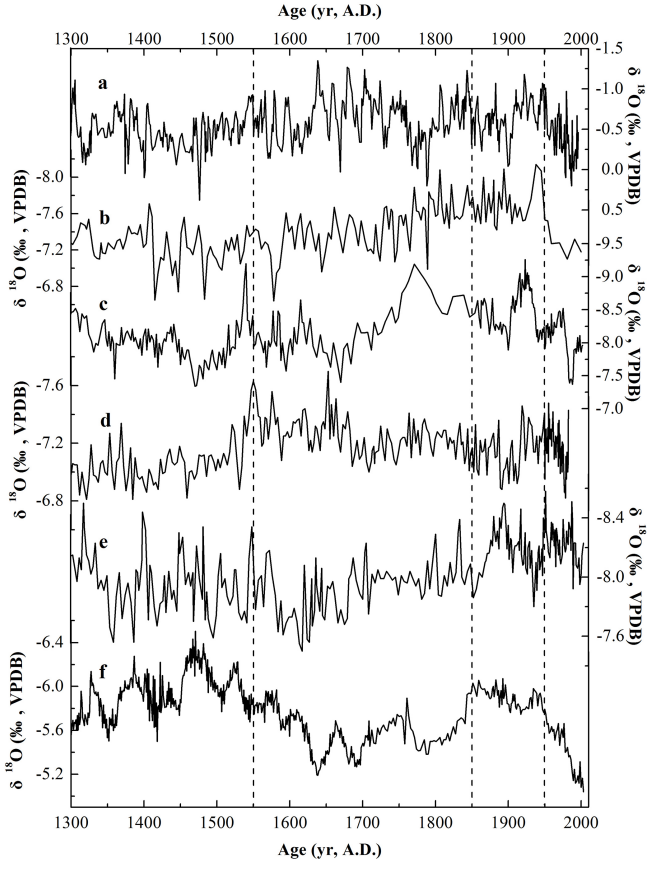

Figure 14. Comparison of δ^{18}O record of stalagmite LHD1 with other speleothem records in the Asian monsoonal region. **(a)** S3 record from Defore Cave, Oman, **(b)** DA record from Dongge Cave, China, **(c)** HS-4 record from Heshang Cave, China, **(d)** DY-1 record from Dayu Cave, China, **(e)** WX42B record from Wanxiang Cave, China, and **(f)** LHD1 record (this study). The locations of these Chinese caves were marked in Fig. 1.

Jiuxian Cave records (Cai et al., 2010). These results (from spectrum analysis) support the link of Asian monsoon rainfall to solar activity and ENSO.

4.3 Comparison of speleothem records in the Asian monsoonal region

Since the late 1990s, numerous speleothem records have been generated. On millennial to orbital scales, many speleothem records from the monsoonal regions are comparable, as the dominant factors influencing the summer monsoon strength were changes in solar insolation and major ocean circulation. Although our study indicates that variations of solar irradiation, air temperature and ENSO conditions are important forcing factors to influence the Asian monsoonal climates on decadal to centennial scales, whether speleothem records on such timescales are comparable remains the question. Here we put some available high-resolution speleothem records from the Asian monsoonal regions together, including the S3 record from Defore Cave in Oman (Burns et al., 2002), DA record from Dongge Cave (Wang et al., 2005), HS-4 record from Heshang Cave (Hu et al., 2008), DY-1 record from Dayu Cave (Tan et al., 2009), WX42B record from Wanxiang Cave (Zhang et al., 2008) and LHD1 record (this study) (Fig. 14). These records were well dated, with an age uncertainty of generally less than 50 years. From the comparison in Fig. 14, it is difficult to see consistent trends either on decadal scale or centennial scale over entire eastern China. In fact, on annual-to-centennial scales, forcing factors of monsoonal variability are more and further complicated. Considering that the eastern China monsoonal region is a broad area with complicated geographical settings, the summer monsoon rain has strong spatial disparity. For instance, as the previous section has demonstrated before, a stronger Asian summer monsoon is not necessary to produce high summer quarter rainfall (Fig. 11). It has been evident that stronger EASM will result in higher summer

rainfall in northern China, but lower summer rainfall in the lower and middle reaches of the Yangtze River (Zhang et al., 2010; Chu et al., 2012). Changes in the δ^{18}O of monsoonal moisture source may also depend on location. Therefore, on annual- to centennial scales, stalagmite δ^{18}O records from different regions over eastern China are not necessarily uniform. In order to understand paleo-monsoonal climates over eastern China, more well-dated and high-resolution records from different locations need to be reconstructed.

5 Conclusions

The well-dated, high-resolution δ^{18}O record of aragonite stalagmite LHD1 from Lianhua Cave in the Wuling Mountain area, central China since 1300 has been compared with instrumental weather records, historic dry–wet index, eastern China temperature, solar irradiation and ENSO variation. The δ^{18}O record on decadal- to centennial scales reflects mainly changes in local dry–wet conditions and monsoonal moisture sources, which are closely related to the summer monsoon intensity. An intensified summer monsoon under high continental temperature caused by enhanced solar irradiation will provide wetter conditions in central China, resulting in lighter δ^{18}O execution in LHD1 record. During cold stages, ENSO variation becomes a major factor to influence the East Asian summer monsoon, with weak summer monsoons under El Niño conditions and strong monsoons under La Niña conditions. Spectrum analysis of the LHD1 δ^{18}O record appears to demonstrate cyclicities of 2–4 and 47 years, indicating the summer monsoon intensity link to solar activity and ENSO variation. In the study area of central China, the summer quarter/spring quarter rainfall ratio is a potential indicator of the EASM strength, with the lower ratio reflecting stronger EASM, which results in higher annual rainfall and lighter δ^{18}O of monsoonal moisture from the Indian Ocean. On annual- to centennial scales, speleothem δ^{18}O records over the monsoonal region cannot be consistent due to multiple forcing factors on the summer monsoon intensity, complicated geographical settings and regional disparity of monsoonal rain. One may not accept the use of a single speleothem record to interpret monsoonal climates over the vast eastern China. The LHD1 δ^{18}O record shows that on centennial scales, warmer and wetter conditions prevailed during 1300–1550 and 1850–1950 in the Wuling Mountain area. During 1550–1850 of the LIA, climate in the Wuling Mountain area was cold and dry. On decadal scales, drought events occurred in ca. 1350, 1420, 1450, 1500, 1550, 1590, 1620, 1640, 1690, 1735, 1760, 1785, 1855, 1877 and 1890.

The Supplement related to this article is available online at doi:10.5194/cp-10-1803-2014-supplement.

Acknowledgements. This project was supported by grants from the geological survey program of the Ministry of Land and Resource of China (Granted No. 12120113006700), China Scholar Council (Granted No. 201206990052), National Science Foundation of China (Granted No. 41072192). Grants from NSC101-2116-M-002-007 and 102-2811-M-002-177 to H.-C. Li supported stable isotope analyses. NSFC (41230524) to H. Cheng and NSFC (41172165) to T.-Y Li are also acknowledged. Thanks to Rich Knurr for the XRD analysis in the Department of Earth Sciences at the University of Minnesota. We also thank Yanbin Lu, Julie Retrum and Mellissa Cross for their help with U-Th dating in University of Minnesota. Aoyu Wang, Guangde Zhu and Guansheng Xiang are acknowledged for their help with field work.

Edited by: M.-T. Chen

References

Bond, G., Kromer, B., Beer, J., Muscheler, R., Evans, M. N., Showers, W., Hoffmann, S., Lotti-Bond, R., Hajdas, I., and Bonani, G.: Persistent solar influence on North Atlantic climate during the Holocene, Science, 294, 2130–2136, 2001.

Broecker, W. S. and Putnam, A. E.: Hydrologic impacts of past shifts of earth's thermal equator offer insight into those to be produced by fossil fuel CO_2, P. Natl. Acad. Sci., 110, 16710–16715, 2013.

Burns, S. J., Fleitmann, D., Mudelsee, M., Neff, U., Matter, A., and Mangini, A.: A 780-year annually resolved record of Indian Ocean monsoon precipitation from a speleothem from south Oman, J. Geophys. Res., 107, 4434, doi:10.1029/2001JD001281, 2002.

Cai, Y., Tan, L., Cheng, H., An, Z., Edwards, R. L., Kelly, M. J., Kong, X., and Wang, X.: The variation of summer monsoon precipitation in central China since the last deglaciation, Earth Planet. Sc. Lett., 291, 21–31, 2010.

Cheng, H., Edwards, R. L., Broecker, W. S., Denton, G. H., Kong, X., Wang, Y., Zhang, R., and Wang, X.: Ice age terminations, Science, 326, 248–252, 2009.

Cheng, H., Sinha, A., Wang, X., Cruz, F. W., and Edwards, R. L.: The global paleomonsoon as seen through speleothem records from Asia and the Americas, Clim. Dynam., 39, 1045–1062, 2012.

Cheng, H., Edwards, R. L., Shen, C.-C., Polyak, V. J., Asmerom, Y., Woodhead, J., Hellstrom, J., Wang, Y., Kong, X., Spötl, C., Wang, X., and Alexander Jr., E. C.: Improvements in ^{230}Th dating, ^{230}Th and ^{234}U half-life values, and U-Th isotopic measurements by multi-collector inductively coupled plasma mass spectrometry, Earth Planet. Lett., 371–372, 82–91, 2013.

Chinese Academy of Meteorological Sciences (CAM): Yearly Charts of Dryness/Wetness in China for the Last 500-Year Period, Beijing, SinoMap Cartogr. Publ. House, Beijing, 1981 (in Chinese).

Chu, P. C. Li, H.-C., Fan, C.-W., Chen, Y.-H.: Speleothem Evidence for Temporal-Spatial Variation in East Asian Summer Monsoon since Medieval Warm Period, J. Quaternary Sci., 27, 901–910, 2012.

Cook, E. R., D'Arrigo, R. D., and Anchukaitis, K. J.: ENSO reconstructions from long tree-ring chronologies: Unifying the differences, in: Talk presented at a special workshop on Reconciling ENSO Chronologies for the Past 500 Years, held in Moorea, French Polynesia on 2–3 April 2008, 2008.

Cook, E. R., Anchukaitis, K. J., Buckley, B. M., D'Arrigo, R. D., Jacoby, G. C., and Wright, W. E.: Asian monsoon failure and megadrought during the last millennium, Science, 328, 486–489, 2010.

Cosford, J., Qing, H., Eglington, B., Mattey, D., Yuan, D., Zhang, M., and Cheng, H.: East Asian monsoon variability since the Mid-Holocene recorded in a high-resolution, absolute-dated aragonite speleothem from eastern China, Earth Planet. Sc. Lett., 275, 296–307, 2008.

Cosford, J., Qing, H., Mattey, D., Eglington, B., and Zhang, M.: Climatic and local effects on stalagmite δ^{13}C values at Lianhua Cave, China. Palaeogeogr. Palaeocl. 280, 235–244, 2009.

Cui, Y. F., Wang, Y. J., Cheng, H., Zhao, K., and Kong, X. G.: Isotopic and lithologic variations of one precisely-dated stalagmite across the Medieval/LIA period from Heilong Cave, central China, Clim. Past, 8, 1541–1550, doi:10.5194/cp-8-1541-2012, 2012.

Delaygue, G. and Bard, E.: An Antarctic view of Beryllium-10 and solar activity for the past millennium, Clim. Dynam., 36, 2201–2218, 2011.

Dorale, J. A. and Liu, Z.-H.: Limitations of hendy test criteria in judging the paleoclimatic suitability of speleothems and the need for replication, J. Cave Karst Stud., 71, 73–80, 2009.

Dykoshi, C. A., Edwards, R. L., Cheng, H., Yuan, D., Cai, Y., Zhang, M., Lin, Y., Qin, J., An, Z., and Revenaugh, J.: A high-resolution, absolute-dated Holocene and deglacial Asian monsoon record from Dongge Cave, China, Earth Planet. Sc. Lett., 233, 71–86, 2005.

Edwards, R. L., Chen, J. H., and Wasserburg, G. J.: ^{238}U-^{234}U-^{230}Th-^{232}Th systematics and the precise measurement of time over the past 500,000 years, Earth Planet. Sc. Lett., 81, 175–192, 1987.

Fairchild, I. J., Smith, C. L., Baker, A., Fuller, L., Spotl, C., Mattey, D., and McDermott, F.: Modification and preservation of environmental signals in speleothems, Earth-Sci. Rev., 75, 105–153, 2006.

Hendy, C. H.: The isotopic geochemistry of speleothems: 1. The calculation of the effects of different modes of formation on the isotopic composition of speleothems and their applicability as paleoclimatic indicators, Geochim. Cosmochim. Ac., 35, 801–824, 1971.

Hu, C., Henderson, G. M., Huang, J., Xie, S., Sun, Y., and Johnson, K. R.: Quantification of Holocene Asian monsoon rainfall from spatially separated cave records, Earth Planet. Sc. Lett., 266, 221–232, 2008.

IPCC: Climate Change 2007 – The Physical Science Basis, Cambridge Univ. Press, New York, p. 299, 2007.

Jaffey, A. H., Flynn, K. F., Glendenin, L. E., Bentley, W. C., and Essling, A. M.: Precision measurement of half-lives and specific activities of ^{235}U and ^{238}U, Phys. Rev. C, 4, 1889–1906, 1971.

Johnson, K. R. and Ingram, B. L.: Spatial and temporal variability in the stable isotope systematics of modern precipitation in China: implications for paleoclimate reconstructions, Earth Planet. Sc. Lett., 220, 365–377, 2004.

Kelly, M. J., Edwards, R. L., Cheng, H., Yuan, D., Cai, Y., Zhang, M., Lin, Y., and An, Z.: High resolution characterization of the Asian monsoon between 146,000 and 99,000 years B.P. from Dongge Cave, China and global correlation of events surrounding Termination II, Palaeogeogr. Palaeocl., 236, 20–38, 2006.

Kutzbach, J. E.: Monsoon climate of the early Holocene: climate experiment with the earth's orbital parameters for 9000 years ago, Science, 214, 59–61, 1981.

Lamb, H. H.: Climatic history and the future, Princeton Univ. Press, Princeton, NJ, 835 pp., 1977.

Li, H.-C., Ku, T.-L., Stott, L. D., and Chen, W.-J.: Applications of interannual- resolution stable isotope records of speleothem: Climatic changes in Beijing and Tianjin, China during the past 500 years – the δ^{18}O record, Sci. China Ser. D, 41, 362–368, 1998.

Li, H.-C., Yuan, D.-X., Ku, T.-L., Wan, N.-J., Ma, Z.-B., Zhang, P.-Z., Bar-Matthews, M., Ayalon, A., Liu, Z.-H., Zhang, M.-L., Zhu, Z.-Y., and Wang, R.-M.: Stable Isotopic Compositions of Waters in the Karst Environments of China: Climatic Implications, Appl. Geochem., 22, 1748–1763, 2007.

Li, H.-C., Lee, Z.-H., Wan, N.-J., Shen, C.-C., Li, T.-Y., Yuan, D.-X., and Chen, Y.-H.: Interpretations of δ^{18}O and δ^{13}C in aragonite stalagmites from Furong Cave, Chongqing, China: A 2000-year record of monsoonal climate, J. Asian Earth Sci., 40, 1121–1130, 2011.

Liu, J., Song, X., Yuan, G., Sun, X., Liu, X., and Wang, S.: Characteristics of δ^{18}O in precipitation over Eastern monsoon China and the water vapor sources, Chinese Sci. Bull., 55, 200–211, 2010.

Liu, Z., Wen, X., Brady, E. C., Otto-Bliesner, B., Yu, G., Lu, H., Cheng, H., Wang, Y., Zheng, W., Ding, Y., Edwards, R. L., Cheng, J., Liu, W., and Yang, H.: Chinese cave records and the East Asia Summer Monsoon, Quaternary Sci. Rev., 83, 115–128, 2014.

Matthes, F. E.: Report of the committee on glaciers, Transactions of the American Geophysical Union, 1939, 518–523, 1939.

McDermott, F.: Palaeo-climate reconstruction from stable isotope variations in speleothems: a review, Quaternary Sci. Rev., 23, 901–918, 2004.

PAGES 2k Consortium: Continental-scale temperature variability during the past two millennia, Nat. Geosci., 6, 339–346, 2013.

Pausata, F. S. R., Battisti, D. S., Nisancioglu, K. H., and Bitz, C. M.: Chinese stalagmite δ^{18}O controlled by changes in the Indian monsoon during a simulated Heinrich event, Nat. Geosci. 4, 474–480, 2011.

Qian, W.-H., Lin, X., Zhu, Y.-F., Xu, Y., and Fu, J.-L.: Climatic regime shift and decadal anomalous events in China, Clim. Change, 84, 167–189, 2007.

Schulz, M. and Mudelsee, M.: REDFIT: estimating red-noise spectra directly from unevenly spaced paleoclimatic time series, Comput. Geosci., 28, 421–426, 2002.

Shi, F., Yang, B., and Von Gunten, L.: Preliminary multiproxy surface air temperature field reconstruction for China over the past millennium, Sci. in China Ser. D, 55, 2058–2067, 2012.

Tan, L., Cai, Y., Cheng, H., An, Z., and Edwards, R. L.: Summer monsoon precipitation variations in central China over the past 750 years derived from a high-resolution absolute-dated stalagmite, Palaeogeogr. Palaeocl., 280, 432–439, 2009.

Tan, M.: Climatic differences and similarities between Indian and East Asian Monsoon regions of China over the last millennium: a perspective based mainly on stalagmite records, Int. J. Speleol., 36, 75–81, 2007.

Tan, M.: Trade-wind driven inverse coupling between stalagmite δ^{18}O from monsoon region of China and large scale temperature – circulation effect on decadal to precessional timescales, Quaternary Sci. 31, 1086–1097, doi:10.3969/j.issn.1001-7410.2011.06.16, 2011 (in Chinese).

Tao, S. Y., Fu, C. B., Zeng, Z. M., and Zhang Q. Y.: Two Long-Term Instrumental Climatic Data Bases of the People's Republic of China. Environmental Sciences Division, Carbon Dioxide Information Analysis Center, Oak Ridge National Laboratory, Oak Ridge, Tennessee, USA, Publication No. 4699, 1997.

Thorrold, S. R., Campana, S. E., Johns, C. M., and Swart, P. K.: Factors determining δ^{13}C and δ^{18}O fractionation in aragonitic otoliths of marine fish, Geochim. Cosmochim. Ac., 61, 2909–2919, 1997.

Wan, N.-J., Li, H.-C., Liu, Z.-Q., and Yuan, D.-X.: Spatial variations of monsoonal rain in eastern China: Instrumental, historic and speleothem records, J. Asian Earth Sci., 40, 1139–1150, 2011.

Wang, B.: The Asian Monsoon, Springer Praxis Publishing, Chichester, UK, 787 pp. ISBN: 3-540-40610-7, 2006.

Wang, S., Wen, X., Luo, Y., Dong, W., Zhao, Z., and Yang, B.: Reconstruction of temperature series of China for the last 1000 years, Chinese Sci. Bull., 52, 3272–3280, 2007.

Wang, Y. J., Cheng, H., Edwards, R. L., An, Z. S., Wu, J. Y., Shen, C.-C., and Dorale, J. A.: A high-resolution absolute-dated late Pleistocene monsoon record from Hulu Cave, China, Science, 294, 2345–2348, 2001.

Wang, Y., Cheng, H., Edwards, R. L., He, Y., Kong, X., An, Z., Wu, J., Kelly, M. J., Dykoski, C. A., and Li, X.: The Holocene Asian monsoon: links to solar changes and North Atlantic climate, Science, 308, 854–857, 2005.

Wang, Y., Cheng, H., Edwards, R. L., Kong, X., Shao, X., Chen, S., Wu, J., Jiang, X., Wang, X., and An, Z.: Millennial- and orbital-scale changes in the East Asian monsoon over the past 224,000 years, Nature, 451, 1090–1093, 2008.

Zhang, D. E., Li, X. Q., and Liang, Y. Y.: Continuation (1992–2000) of the yearly charts of dryness/wetness in China for the last 500 years period, J. Appl. Meteorol. Sci., 14, 379–388, 2003 (in Chinese).

Zhang, D. E.: Severe drought events as revealed in the climate records of China and their temperature situations over the last 1000 years, Acta Meteorol. Sin., 19, 485–491, 2005.

Zhang, D. E., Li, H.-C., Ku, T.-L., and Lu, L.-H.: On Linking Climate to Chinese Dynastic Change: Spatial and Temporal Variations of Monsoonal Rain, Chinese Sci. Bull., 55, 77–83, 2010.

Zhang, H.-L., Yu, K.-F., Zhao, J.-X., Feng, Y.-X., Lin, Y.-S., Zhou, W., and Liu, G.-H..: East Asian summer monsoon variations in the past 12.5 ka: high-resolution δ^{18}O record from a precisely dated aragonite stalagmite in central China, J. Asian Earth Sci., 73, 162–175, 2013.

Zhang, P., Cheng, H., Edwards, R. L., Chen, F., Wang, Y., Yang, X., Liu, J., Tan, M., Wang, X., Liu, J., An, C., Dai, Z., Zhou, J., Zhang, D., Jia, J., Jin, L., and Johnson, K. R.: A test of climate, sun, and culture relationships from an 1810-year Chinese cave record, Science, 322, 940–942, 2008.

Zhou, T.-J. and Yu, R.-C.: Atmospheric water vapor transport associated with typical anomalous summer rainfall patterns in China, J. Geophys. Res., 110, D08104, doi:10.1029/2004JD005413, 2005.